Published in final edited form as:
J Alzheimers Dis. 2013 ; 35(4): 777–788. doi:10.3233/JAD-122419.

Brain Transit and Ameliorative Effects of Intranasally Delivered Anti-Amyloid-β Oligomer Antibody in 5XFAD Mice

Chun Xiao[a,b], **Francesca J. Davis**[a,b], **Balwantsinh C. Chauhan**[c], **Kirsten L. Viola**[d,e], **Pascale N. Lacor**[d,e], **Pauline T. Velasco**[d], **William L. Klein**[d,e], and **Neelima B. Chauhan**[a,b,*]

[a]Neuroscience Research, Jesse Brown VA Medical Center, Chicago, IL, USA

[b]Department of Pediatrics, University of Illinois Hospital & Health Science System-Children's Hospital, University of Illinois at Chicago, Chicago, IL, USA

[c]Department of Biopharmaceutical Sciences, Roosevelt University, Schaumburg, IL, USA

[d]Department of Neurobiology, Northwestern University, Evanston, IL, USA

[e]Cognitive Neurology & Alzheimer's Disease Center, Northwestern University, Chicago, IL, USA

Abstract

Alzheimer's disease (AD) is a global health crisis with limited treatment options. Despite major advances in neurotherapeutics, poor brain penetration due to the blood-brain barrier continues to pose a big challenge in overcoming the access of therapeutics to the central nervous system. In that regard, the non-invasive intranasal route of brain targeting is gaining considerable attention. The nasal mucosa offers a large surface area, rapid absorption, and avoidance of first-pass metabolism increasing drug bioavailability with less systemic side effects. Intranasal delivery is known to utilize olfactory, rostral migratory stream, and trigeminal routes to reach the brain. This investigation confirmed that intranasal delivery of oligomeric amyloid-β antibody (NU4) utilized all three routes to enter the brain with a resident time of 96 hours post single bolus intranasal administration, and showed evidence of perikaryal and parenchymal uptake of NU4 in 5XFAD mouse brain, confirming the intranasal route as a non-invasive and efficient way of delivering therapeutics to the brain. In addition, this study demonstrated that intranasal delivery of NU4 antibody lowered cerebral amyloid-β and improved spatial learning in 5XFAD mice.

Keywords

Alzheimer's immunotherapy; amyloid-β oligomer antibody; brain transit; cerebral amyloid-β immunocytochemistry; intranasal delivery; olfactory pathway; rostral migratory stream pathway; spatial acquisition learning; trigeminal pathway

INTRODUCTION

Despite enormous advances in the field of brain research, central nervous system (CNS) disorders, such as Alzheimer's disease (AD), remain the world's leading cause of mental disability and demise [1]. AD is a devastating incurable disease currently afflicting >5

*Correspondence to: Neelima B. Chauhan, Ph.D., Jesse Brown VA Medical Center, 820 South Damen Avenue, Chicago, IL 60612, USA. Tel.: +1 312 569 7747; Fax: +1 312 569 8114; nchauhan@uic.edu.

Authors' disclosures available online (http://www.j-alz.com/disclosures/view.php?id=1688).

million Americans, with the projected escalation to >16 million by 2050 if effective disease-modifying treatments are not discovered [2, 3].

Based on the widely accepted concept of overproduction and deposition of amyloid-β peptide (Aβ) as a key seeding event in AD pathogenesis [4, 5], removal of Aβ by immunotherapeutic strategies continues to be one of the promising strategies in treating AD [6, 7]. Antibodies to Aβ derived from active or passive immunizations have been shown to reduce cerebral Aβ and Aβ-associated toxicity as well as improve cognitive deficits in AD [8–11]. Although partially successful, all immunization strategies explored thus far have various limitations. Passive immunization using anti-Aβ antibodies directly delivered to the brain via intracranial route have shown greater benefits than indirect access of anti-Aβ antibodies derived from active or systemic passive immunization strategies [12–14]. However, direct delivery of antibodies to the brain via an intracranial route is potentially limited due to its invasiveness. In that regard, intranasal route of direct drug delivery to the brain is increasingly gaining interest as a non-invasive and safe approach to target therapeutics directly to the brain [15, 16]. Many drugs administered intranasally, such as Exendin-4 [17], Losartan [18], insulin/insulin-like growth factor-1 [19–23], nerve growth factor [24–27], and brain-derived neurotrophic factor [28–30], have been able to reach the CNS and exert therapeutic effects. Surprisingly, there are very few studies showing intranasal delivery of antibody [31, 32], particularly in relation to AD [33, 34].

Intranasal administration is known to utilize three major pathways to deliver administered material to the brain including the olfactory [35–38], rostral migratory stream (RMS) [39, 40], and trigeminal [15, 36, 41] routes. Current investigation examined which of these known (olfactory, RMS, and trigeminal) pathways are involved in the transfer of anti-oligomeric Aβ antibody (NU4) when delivered intranasally, and if intranasally delivered NU4 exhibited neuronal uptake in 5XFAD mice modeling AD. In addition, this study examined if intranasally delivered NU4 is efficient in lowering cerebral Aβ and in improving cognition in 5XFAD mice.

MATERIALS AND METHODS

5XFAD transgenic mice harboring mutations in amyloid-β protein precursor (AβPP) (K670N/M671L + I716V + V717I) and presenilins (PS1/2) (M146L + L286V) genes [42], were bred by crossing 5XFAD heterozygous male(s) (original breeder males obtained from Dr. Vassar, Northwestern University, Chicago, IL), with C57/B6 F1 females (Jackson Labs, Bar harbor, ME). Presence of transgene was identified by PCR genotyping of tail genomic DNA with specific forward and reverse primers (Eurofins, Operon). All animal procedures were performed in accordance with the Jesse Brown VA Medical Center institutional Animal Care and Use Committee approval, and National Research Council's guidelines.

5XFAD mice were divided into 3 major groups (n = 6/group). Mice were anesthetized with Ketamine (100 mg/kg, i.p.) and Xylazine (10 mg/kg, i.p.) and held in an upright position to maximize intranasal (IN) access of IN-administered material while simultaneously minimizing extra-nasal entry in the surrounding areas such as the throat (Fig. 1A). With the use of a micropipette (Fig. 1B), mice were IN administered either with a single bolus dose of sterile saline vehicle (5 μl/naris, Total 10 μl) (Group 1); or horseradish peroxidase (HRP)-labeled anti-oligomer Aβ antibody (NU4) (HRP-NU4) (Alpha Diagnostics, San Antonio, TX) (5 μg/5 μl/naris; Total 10 μg/10 μl) (Group 2); or Alexa 568-labeled NU4 (Alexa-NU4) (5 μg/5 μl/naris; Total 10 μg/10 μl) (Group 3). NU4 antibody was conjugated with Alexa Fluor® 568 using the Alexa Fluor® 568 Protein Labeling Kit (Invitrogen) according to manufacturer's instructions with a minor modification. PBS buffer provided was replaced with 10×PBS (0.1 M potassium phosphate, 1.5 M NaCl, pH 7.2) without sodium azide to

avoid complications with IN injection later. Antibody was stored frozen at −80°C until needed.

HRP-labeled IN injected groups were allowed to survive for 2, 6, 12, 24, 36, or 96 h post-injection while Alexa-NU4 injected groups were allowed to survive for 6 and 12 h post-injection. Mice were euthanized at the end of each respective treatment, and brains were harvested, snap frozen, processed to obtain frozen sagittal sections of 40 μm thickness, and lightly fixed with formaldehyde post-sectioning. The brain sections from mice injected with saline (Fig. 3) as well as HRP-labeled NU4 antibody (Figs. 4 and 5) were subjected to standard diaminobenzidine chromogen development to reveal HRP label, and counterstained with Nissl nuclear label to visualize microscopic topography of the brain. The brain sections from mice injected with fluorescently labeled NU4 were mounted using Prolong anti-fade reagent containing DAPI (blue) to labeled cell nuclei of the various brain regions (Fig. 6).

HRP-NU4 injected mice were used to track major cerebral routes, i.e., olfactory pathway (Fig. 2, blue & red arrows), RMS pathway (Fig. 2, yellow arrowheads), and trigeminal pathway (Fig. 2, purple arrows) after IN administration. Alexa-NU4 injected mice were used to confirm brain uptake of IN injected antibody. Sections were subjectively observed by 3 independent investigators. Images were captured on Olympus BX series microscope using ImagePro. Fluorescent images were captured using a Leica confocal microscope.

Another set of experiments was conducted to test the efficacy of IN-delivered NU4 antibody in decreasing cerebral amyloid and in improving cognitive functions in 5XFAD mice. Mice were divided into 4 major groups (n = 5/group) as follows:

Group 1 2-month-old 5XFAD untreated controls IN administered with 10 μl of sterile saline at the treatment start point only once, tested for spatial learning, euthanized, and 10 μm-thick brain sections analyzed for Aβ immunocytochemistry.

Group 2 2-month-old 5XFAD experimental mice IN administered with NU4 antibody [(10 μg/5 μl/naris) = (20 μg/mouse); twice/ week; 40 μg/mouse/ week] for 8 weeks. At the end, these 4-month-old experimental transgenic mice were tested for spatial learning, euthanized, and 10 μm-thick brain sections analyzed for Aβ immunocytochemistry.

Group 3 2-month-old 5XFAD untreated age-matched controls IN administered with an equal volume of sterile saline (5 μl/ naris, 10 μl/once, twice/week) for 8 weeks. At the end, these 4-month-old untreated age-matched control transgenic mice that received IN saline for 8 weeks in parallel to IN NU4 treatment were tested for spatial learning, euthanized, and 10 μm-thick brain sections analyzed for Aβ immunocytochemistry.

Group 4 2-month-old non-transgenic age-matched littermate controls IN administered with an equal volume of sterile saline (5 μl/ naris, 10 μl/once, twice/week) for 8 weeks. At the end, these 4-month-old untreated age-matched littermate controls that received IN saline for 8 weeks in parallel to IN NU4 treatment were tested for spatial learning, euthanized, and 10 μm-thick brain sections analyzed for Aβ immunocytochemistry.

Morris water maze testing for spatial acquisition of place and cue learning was performed as established. Morris water maze is a circular pool of water of 1.4 m diameter filled with water maintained at 25°C. The floor of the pool was divided into imaginary 3 annuli and 4 quadrants. An indiscernible platform made up of transparent acrylic was placed in one of the quadrant, 1 cm below the surface of water. Mice were subjected to experimental trials (6 trials per day for 3 days), admitted in the pool facing the pool wall with a randomly selected

start point on the opposite side of platform quadrant, allowed to swim for a maximum of 60 s to locate the submerged platform. The time required for locating submerged platform is termed as "Latency". Latency for each animal per day was recorded by video tracking (Accuscan) and averaged across number of trials/day. A group mean was derived from individual averages. The data were analyzed by repeated measures analysis of variance (RMANOVA) followed by Tukey *post hoc* test. A value of $p < 0.05$ was considered statistically significant.

Following behavior, the mice were euthanized as follows. Animals were sedated using CO_2 inhalation. After confirming complete sedation, animals were transcardially perfused with sterile saline first to remove all blood, followed by perfusion with 4% buffered paraformaldehyde. Fixed brains were harvested and processed for paraffin embedding and sectioning. 10 μm-thick paraffin sections were used to perform immunocytochemistry using 6E10 antibody (antibody raised against 1–16 amino acid residues of Aβ, Covance) to detect cerebral Aβ plaques deposited within the brain parenchyma, as detailed below.

Briefly, sections were deparaffinized, hydrated, and washed in a wash solution (10 mM Tris-HCl (pH 7.6), 0.5% bovine serum albumin, and 0.87% NaCl), 3 times for 5 min each. After this step, all incubations were performed in a humid chamber: (a) 5% non-immune host serum (in which the primary antibody is made) for 60 min; (b) Optimal dilution (1 : 1000) of primary antibody (6E10) diluted with antibody dilution buffer (10 mM Tris-HCl (pH 7.6), 0.5% goat serum, and 0.1% Triton X100), for 18–20 h; (c) Washed in wash solution; (d) AlexaFluor594 conjugated goat antimouse IgG diluted 1 : 100 with antibody dilution buffer, and washed as in (c); and mounted in anti-fade mounting medium. Procedural controls consisted of omission of primary antiserum (omit controls). Immunofluorescent cortical plaques were quantitated with the use of ImagePro/ImageJ imaging system using Olympus BX41 series microscope with CCD camera. Following background correction, sections were sampled for quantitating 6E10 immunoreactivity within the defined high power fields of cerebral cortex bilaterally. Five high power fields from each unilateral cerebral cortex were averaged to obtain individual values. Individual values were used to obtain group means and analyzed by ANOVA to determine main effect of the treatment across the groups, followed by Tukey *posthoc* test for comparisons between control and experimental groups. A value of $p < 0.05$ was considered statistically significant.

RESULTS

Transit of HRP-labeled NU4 in the brains of 5XFAD mice

Compared to the saline vehicle injected brains that did not reveal any HRP labeling (Fig. 3A, B), a single bolus IN injection of HRP-labeled NU4 (HRP-NU4) was observed to enter the brain immediately within 2 h post injection. IN-injected material transited throughout the brain parenchyma within 6–12 h post injection (Fig. 4), and was retained in respective brain areas up to 24, 36, and 96 h post injection within the brain parenchyma (time-points 24 h and beyond not shown to avoid redundancy). It was interesting to note that even at the post-injection time point of 96 h, the injected antibody was still detected in the brain in traces, indicating a maximum resident time of 96 h post single bolus IN administration of NU4 antibody.

Observations at different post injection time points indicated that by 2 h, NU4 passed through the glomerular and plexiform layers of the olfactory epithelium and entered the microvasculature of the olfactory tract (Fig. 4B, C, arrows). Advanced progression of the antibody was clearly evident at 6 h post injection showing profusely labeled microvasculature of the olfactory tract (Fig. 4D, arrow), and progression of HRP-NU4 transit in this tract (Fig. 4E, arrow).

With regard to the penetration of IN-injected antibody into the accessory olfactory bulb (AOB) and RMS path, it was observed that within the window of 2–6 h post injection, the antibody penetrated into the AOB (Fig. 4F, arrowhead) and entered the RMS (Fig. 4F, arrow) with further progression in RMS (Fig. 4G, arrow). Within the next 6 h (12 h post injection), the antibody reached the hippocampus (Fig. 4H, arrows) and its surrounding parenchyma (Fig. 4I, arrows). The detection of HRP-NU4 within the olfactory-trigeminal path (Fig. 4K, arrows) leading to the 4th ventricle (Fig. 4J, arrows) was also observed at 12 h post injection. Thus, IN-injected antibody was found to penetrate the brain within 2 h post injection, spread throughout the brain within 12 h post injection, and was retained up to 24 and 36 h. A trace of HRP label was still observed 96 h post injection.

Brain uptake of NU4 in 5XFAD mice

Detection of HRP-NU4 within the brain parenchyma was observed as early as 6 h post injection in the vicinity of the 3rd ventricle (Fig. 5A, arrows), midbrain (Fig. 5B, arrows), and hippocampus (Fig. 5C, arrows). High power magnification indicated perikaryal localization of NU4 (Fig. 5D, arrowheads).

Observation under confocal microscopy revealed that IN-administered NU4 antibody (red) diffused away from the injection site and was found to be localized in the glomerular layer of the olfactory bulb, the isocortex, and the hippocampus. As early as 6 h after injection, NU4 was found in the olfactory bulb (Fig. 6, OB-6 h). Later time showed much less NU4 labeling suggesting a clearance from the olfactory bulb (Fig. 6, OB-12 h). NU4 antibody was detected in the hippocampus as early as 6 h (not shown) but the abundance of the NU4 deposits was greatly increased in the 12 h group compared to 6 h (Fig. 6, Hippocampus). Detection of NU4 was particular evident in the pyramidal cell layer of the hippocampal CA1 region. NU4 labeling appeared around cell bodies (Fig. 6, panel 1) and higher magnification was found to be reminiscent of the perisomatic distribution described in Lacor et al. [43]. Additionally, individual puncta were detectable throughout the neuropil where dendritic processes are abundant (Fig. 6, panel 2). NU4 antibody was also observed intracellularly in cortical areas.

With regard to the amyloid lowering effects of IN-administered NU4, the results showed that there was a progressive build-up of 6E10-immunoreactive (IR) Aβ plaques from 2 to 4 months of age in the brains of 5XFAD mice without any treatment (Fig. 7, compare B to C). IN immunization with NU4 remarkably reduced cerebral plaque burden in 5XFAD mice, as evidenced by reduced 6E10-IR Aβ plaque distribution in immunized transgenics (Fig. 7D). Densitometric quantitation confirmed this observation indicating that compared to the control littermates, the deposition of 6E10-IR Aβ plaques increased by ~10-fold in the brains of 2-month-old saline injected untreated control transgenic mice. From 2 to 4 months of age, the plaque build-up further increased by additional ~2.5-fold increased deposition of 6E10-IR Aβ plaques in the brains of 4-month-old saline injected age-matched untreated control transgenics (Fig. 8, all values, $p < 0.0001$). IN immunization using NU4 significantly reduced 6E10-IR Aβ plaques by 1.4-fold in the brains of 4-month-old immunized 5XFAD mice, compared to 4-month-old saline injected age-matched untreated control transgenic mice (Fig. 8, all values, $p < 0.0001$).

Parallel to the amyloid-lowering effects, the spatial acquisition learning was found to be improved in 5XFAD mice after IN immunization using NU4 antibody. Effect of IN immunization on spatial acquisition learning in 5XFAD mice was measured by a spatial learning task using Morris water maze apparatus in which the animal is trained to learn a location of the submerged platform in a pool of water. The learning trials are judged by the latency (time in seconds required to reach the submerged platform in a given trial of 60 s duration). As seen in Fig. 9, minimum latencies (8–15 s) were required by non-transgenic

littermate controls, while transgenic control mice exhibited progressively greater latencies from 2-months (15–18 s) to 4-months of age (25–31 s), indicating respective deterioration of spatial learning by 71% (at 2 months) and 89% (at 4 months) in control transgenics. IN immunization with NU4 improved spatial acquisition learning as evidenced by reduced latencies (18–22 s) to reach the submerged platform, indicating 29% of improvement in spatial learning after immunization compared to the age-matched control transgenic mice (all values, $p < 0.0001$).

In summary, the results showed that the IN-injected antibody entered the brain within 2 h post injection with a maximum resident time of 96 h of post single bolus IN administration, displaying perikaryal, perisomal, and parenchymal uptake of IN-injected antibody. Furthermore, the results showed that the transit of IN-injected antibody utilized AOB, RMS, olfactory, and trigeminal pathways. Finally, the results indicated that IN-delivered NU4 antibody efficiently reduced cerebral amyloid and improved spatial acquisition learning in 5XFAD mice.

DISCUSSION

This is the first report showing detailed anatomical brain distribution and uptake of IN-delivered anti-Aβ antibody raised against the most toxic oligomeric species of Aβ(NU4). Conventionally, IN-administered material is taken up by sensory neurons of Gruenberg ganglion and sepal organ projecting to the olfactory epithelium, by ventronasal organ projecting to the AOB, and by olfactory epithelium projecting to the granule cell layer and plexiform layers, eventually draining the IN-administered material into the AOB, RMS, olfactory tract, and trigeminal tract [40, 44, 45]. While the IN-delivered material tracked into the RMS reaches the lateral and 3rd ventricle in the close vicinity of hippocampus [39], the material tracked into the olfactory track from AOB and olfactory lobe delivers material into the midbrain [46], and the material trafficked along the trigeminal track delivers to pons and hind brain, reaching to the 4th ventricle [47].

Currently observed entry of HRP-NU4 right across the glomerular and plexiform layers of olfactory epithelium after 2 h post IN administration of NU4 is consistent with the known facts of NU4 being trafficked through the sensory neurons of Gruenberg ganglion and septal organ projecting to the olfactory epithelium, as well as NU4 directly taken up by olfactory epithelium in the nasal cavity. This transit was further observed to progress along the olfactory tract which appeared to have merged with the trigeminal path as evidenced by detection of HRP-NU4 label at the base of the midbrain. The detection of HRP-NU4 within the 4th ventricle provides additional confirmation of NU4 being trafficked through the trigeminal route as well because it is the trigeminal path that conventionally projects IN-delivered material to the pons, hind brain, and 4th ventricle [41, 44]. On the other hand, detection of HRP-NU4 within the AOB by 6 h post IN-administration confirms the trafficking of IN-delivered NU4 picked up by the septal organ of nasal cavity projecting to AOB, eventually draining into the olfactory path.

The RMS is a specialized migratory route in the brain along which neuronal precursors originating in the subventricular zone of the brain migrate to reach the main olfactory bulb, and thus constitutes a significant part of the olfactory system that stretches from the subventricular zone in the wall of the lateral ventricle, through the basal forebrain, to the olfactory bulb [48]. The importance of the RMS lies in its ability to refine and even change an animal’s sensitivity to smells, which explains its importance and larger size in the rodent brain as compared to the human brain [48]. Although it was originally believed that neurons could not regenerate in the adult brain, neurogenesis has been shown to occur in mammalian brains, including those of primates [49]. However, neurogenesis is limited to the

hippocampus and subventricular zone, and the RMS is one mechanism neurons use to relocate from these areas [50]. In the RMS, vascular cells and astroglia forming gap junctions are arranged parallel to the route of the migrating cells and provide scaffolding [51]. Cells in the RMS are believed to move by “chain migration”. Developing neurons travel toward the olfactory bulb along the RMS via glial tubes, traveling tangential to the brain surface. Researchers tested the role of the RMS in “intranasal delivery of drugs into the CNS” [40]. In this study, the experimenters disrupted the RMS in mice, which obstructed “the uptake of intranasally administered radio-labeled material into the CNS.” Fluorescent tracers were also used to track the medicine throughout the brain. It was found that the medicine spread to all regions of the brain, including the olfactory bulb, concluding that the RMS was extremely prevalent and necessary in the CNS in order to deliver drugs intranasally [40]. In the current investigation, we confirmed the participation of RMS after IN delivery of NU4 in 5XFAD brain, as evidenced by robust uptake and transit of HRP-NU4 within RMS at 6 h post-IN administration, which showed advancing transit along the RMS path, reaching to the 3rd ventricular site in the close vicinity of hippocampus by 12 h post IN-administration.

Mutations in the genes for AβPP and PS1/2 harbored in 5XFAD mice are known to increase production of $A\beta_{42}$ characteristic of familial AD and exhibit expedited plaque development compared to other transgenic mice [42]. 5XFAD mice are known to generate $A\beta_{42}$ very rapidly resulting in amyloid deposition (and gliosis) beginning at ~2 months of age and reaching a very large burden in deep cortical layers. Intraneuronal $A\beta_{42}$ is known to accumulate in 5XFAD brain starting at 1.5 months of age (before plaques get deposited) within the neuron soma and neurites. Parallel to the cerebral Aβ build-up, 5XFAD mice have also shown impaired memory in the Y-maze [42].

Currently observed penetration of NU4 within the brain parenchyma, neuron soma, and neurites certainly appears to have neutralized accumulated Aβ within the neurons and brain parenchyma which resulted in preventing further accumulation of cerebral Aβ, as evidenced by 1.4-fold reduction of 6E10-IR Aβplaques in the brains of 4-month-old 5XFAD mice IN immunized with NU4, compared to 4-month-old saline injected age-matched untreated control transgenics (Figs. 7D and 8). This reduction of cerebral Aβ was observed to be translated in 29% improvement of spatial acquisition learning after immunization (Fig. 9).

Taken together, the current investigation provided anatomical evidence of the involvement of olfactory, RMS, and trigeminal transit routes for anti-oligomer Aβ antibody to enter the brain parenchyma with a resident time of 96 h post single bolus IN administration and showed evidence of perikaryal and perisomal uptake of NU4 in 5XFAD brain, confirming the IN route as a non-invasive and efficient way of administering therapeutics to the brain. In addition, this study confirmed that IN administered NU4 was able to neutralize brain parenchymal Aβ preventing progressive accumulation of cerebral amyloid, resulting in the improvement of spatial acquisition learning-the hippocampal-based cognitive task.

Acknowledgments

This material is the result of work supported with resources and the use of facilities at the Jesse Brown VA Medical Center Chicago, Chicago, IL. The authors acknowledge the support provided by the Westside Institute for Science and Education; Department of Pediatrics, University of Illinois at Chicago, Children’s Hospital of the University of Illinois, Chicago, IL and Department of Biopharmaceutical Sciences, Roosevelt University, Schaumburg, IL. This work has been supported in part by National Institute of Health (AG039625, NBC; AG022547, WLK); by the Alzheimer’s Association (ZEN-09-133875, WLK); and by the Department of Veterans Affairs, Veterans Health Administration, Office of Research and Development, Rehabilitation R&D (B6285R, NBC). The authors also acknowledge the support provided by M.P. Lambert for the generation and purification of NU4 antibody.

References

1. Khachaturian ZS, Petersen RC, Snyder PJ, Khachaturian AS, Aisen P, de Leon M, Greenberg BD, Kukull W, Maruff P, Sperling RA, Stern Y, Touchon J, Vellas B, Andrieu S, Weiner MW, Carrillo MC, Bain LJ. Developing a global strategy to prevent Alzheimer's disease: Leon Thal Symposium 2010. Alzheimers Dement. 2011; 7:127–132. [PubMed: 21414553]
2. Khachaturian ZS, Khachaturian AS. Prevent Alzheimer's disease by 2020: A national strategic goal. Alzheimers Dement. 2009; 5:81–84. [PubMed: 19328433]
3. Bonda DJ, Lee HP, Lee HG, Friedlich AL, Perry G, Zhu X, Smith MA. Novel therapeutics for Alzheimer's disease: An update. Curr Opin Drug Discov Devel. 2010; 13:235–246.
4. Finder VH, Glockshuber R. Amyloid-beta aggregation. Neurodegener Dis. 2007; 4:13–27. [PubMed: 17429215]
5. Kawahara M. Neurotoxicity of beta-amyloid protein: Oligomerization, channel formation, and calcium dyshomeostasis. Curr Pharm Des. 2010; 16:2779–2789. [PubMed: 20698821]
6. Menendez-Gonzalez M, Perez-Pinera P, Martinez-Rivera M, Muniz AL, Vega JA. Immunotherapy for Alzheimer's disease: Rational basis in ongoing clinical trials. Curr Pharm Des. 2011; 17:508–520. [PubMed: 21375481]
7. Holstein GR, Martinelli GP, Friedrich VL. Anatomical observations of the caudal vestibulo-sympathetic pathway. J Vestib Res. 2011; 21:49–62. [PubMed: 21422542]
8. Wisniewski T, Boutajangout A. Vaccination as a therapeutic approach to Alzheimer's disease. Mt Sinai J Med. 2010; 77:17–31. [PubMed: 20101719]
9. Fu HJ, Liu B, Frost JL, Lemere CA. Amyloid-beta immunotherapy for Alzheimer's disease. CNS Neurol Disord Drug Targets. 2010; 9:197–206. [PubMed: 20205640]
10. Pul R, Dodel R, Stangel M. Antibody-based therapy in Alzheimer's disease. Expert Opin Biol Ther. 2011; 11:343–357. [PubMed: 21261567]
11. Zhang Y, Lee DH. Sink hypothesis and therapeutic strategies for attenuating Abeta levels. Neuroscientist. 2011; 17:163–173. [PubMed: 21330304]
12. Chauhan NB, Siegel GJ, Lichtor T. Effect of age on the duration and extent of amyloid plaque reduction and microglial activation after injection of anti-Abeta antibody into the third ventricle of TgCRND8 mice. J Neurosci Res. 2004; 78:732–741. [PubMed: 15478192]
13. Chauhan NB, Siegel GJ. Intracerebroventricular passive immunization in transgenic mouse models of Alzheimer's disease. Expert Rev Vaccines. 2004; 3:717–725. [PubMed: 15606357]
14. Chauhan NB. Intracerebroventricular passive immunization with anti-oligoAbeta antibody in TgCRND8. J Neurosci Res. 2007; 85:451–463. [PubMed: 17086547]
15. Dhuria SV, Hanson LR, Frey WH 2nd. Intranasal delivery to the central nervous system: Mechanisms and experimental considerations. J Pharm Sci. 2010; 99:1654–1673. [PubMed: 19877171]
16. Malerba F, Paoletti F, Capsoni S, Cattaneo A. Intranasal delivery of therapeutic proteins for neurological diseases. Expert Opin Drug Deliv. 2011; 8:1277–1296. [PubMed: 21619468]
17. Kim TH, Park CW, Kim HY, Chi MH, Lee SK, Song YM, Jiang HH, Lim SM, Youn YS, Lee KC. Low molecular weight (1 kDa) polyethylene glycol conjugation markedly enhances the hypoglycemic effects of intranasally administered exendin-4 in type 2 diabetic db/db mice. Biol Pharm Bull. 2012; 35:1076–1083. [PubMed: 22791155]
18. Danielyan L, Klein R, Hanson LR, Buadze M, Schwab M, Gleiter CH, Frey WH. Protective effects of intranasal losartan in the APP/PS1 transgenic mouse model of Alzheimer disease. Rejuvenation Res. 2010; 13:195–201. [PubMed: 20370487]
19. Shemesh E, Rudich A, Harman-Boehm I, Cukierman-Yaffe T. Effect of intranasal insulin on cognitive function: A systematic review. J Clin Endocrinol Metab. 2012; 97:366–376. [PubMed: 22162476]
20. Apostolatos A, Song S, Acosta S, Peart M, Watson JE, Bickford P, Cooper DR, Patel NA. Insulin promotes neuronal survival via the alternatively spliced protein kinase CdeltaII isoform. J Biol Chem. 2012; 287:9299–9310. [PubMed: 22275369]
21. Subramanian S, John M. Intranasal administration of insulin lowers amyloid-beta levels in rat model of diabetes. Indian J Exp Biol. 2012; 50:41–44. [PubMed: 22279939]

22. Kullmann S, Frank S, Heni M, Ketterer C, Veit R, Haring HU, Fritsche A, Preissl H. Intranasal insulin modulates intrinsic reward and prefrontal circuitry of the human brain in lean women. Neuroendocrinology. 2013; 97:176–182. [PubMed: 22922661]

23. Paslakis G, Blum WF, Deuschle M. Intranasal insulin-like growth factor I (IGF-I) as a plausible future treatment of depression. Med Hypotheses. 2012; 79:222–225. [PubMed: 22626951]

24. Covaceuszach S, Capsoni S, Ugolini G, Spirito F, Vignone D, Cattaneo A. Development of a non invasive NGF-based therapy for Alzheimer's disease. Curr Alzheimer Res. 2009; 6:158–170. [PubMed: 19355851]

25. Zhu W, Cheng S, Xu G, Ma M, Zhou Z, Liu D, Liu X. Intranasal nerve growth factor enhances striatal neurogenesis in adult rats with focal cerebral ischemia. Drug Deliv. 2011; 18:338–343. [PubMed: 21348576]

26. Capsoni S, Marinelli S, Ceci M, Vignone D, Amato G, Malerba F, Paoletti F, Meli G, Viegi A, Pavone F, Cattaneo A. Intranasal "painless" human nerve growth factors slows amyloid neurodegeneration and prevents memory deficits in APP X PS1 mice. PLoS One. 2012; 7:e37555. [PubMed: 22666365]

27. Tian L, Guo R, Yue X, Lv Q, Ye X, Wang Z, Chen Z, Wu B, Xu G, Liu X. Intranasal administration of nerve growth factor ameliorate beta-amyloid deposition after traumatic brain injury in rats. Brain Res. 2012; 1440:47–55. [PubMed: 22284619]

28. Jiang Y, Wei N, Lu T, Zhu J, Xu G, Liu X. Intranasal brain-derived neurotrophic factor protects brain from ischemic insult via modulating local inflammation in rats. Neuroscience. 2011; 172:398–405. [PubMed: 21034794]

29. Vaka SR, Murthy SN, Balaji A, Repka MA. Delivery of brain-derived neurotrophic factor via nose-to-brain pathway. Pharm Res. 2012; 29:441–447. [PubMed: 21879386]

30. Zhu J, Jiang Y, Xu G, Liu X. Intranasal administration: A potential solution for cross-BBB delivering neurotrophic factors. Histol Histopathol. 2012; 27:537–548. [PubMed: 22419018]

31. Furrer E, Hulmann V, Urech DM. Intranasal delivery of ESBA105, a TNF-alpha-inhibitory scFv antibody fragment to the brain. J Neuroimmunol. 2009; 215:65–72. [PubMed: 19733918]

32. Ye J, Shao H, Hickman D, Angel M, Xu K, Cai Y, Song H, Fouchier RA, Qin A, Perez DR. Intranasal delivery of an IgA monoclonal antibody effective against sublethal H5N1 influenza virus infection in mice. Clin Vaccine Immunol. 2010; 17:1363–1370. [PubMed: 20668143]

33. Frenkel D, Solomon B. Filamentous phage as vector-mediated antibody delivery to the brain. Proc Natl Acad Sci U S A. 2002; 99:5675–5679. [PubMed: 11960022]

34. Cattepoel S, Hanenberg M, Kulic L, Nitsch RM. Chronic intranasal treatment with an anti-Abeta(30–42) scFv antibody ameliorates amyloid pathology in a transgenic mouse model of Alzheimer's disease. PLoS One. 2011; 6:e18296. [PubMed: 21483675]

35. Thorne RG, Emory CR, Ala TA, Frey WH 2nd. Quantitative analysis of the olfactory pathway for drug delivery to the brain. Brain Res. 1995; 692:278–282. [PubMed: 8548316]

36. Mistry A, Stolnik S, Illum L. Nanoparticles for direct nose-to-brain delivery of drugs. Int J Pharm. 2009; 379:146–157. [PubMed: 19555750]

37. Veronesi MC, Kubek DJ, Kubek MJ. Intranasal delivery of neuropeptides. Methods Mol Biol. 2011; 789:303–312. [PubMed: 21922417]

38. Craft S, Baker LD, Montine TJ, Minoshima S, Watson GS, Claxton A, Arbuckle M, Callaghan M, Tsai E, Plymate SR, Green PS, Leverenz J, Cross D, Gerton B. Intranasal insulin therapy for alzheimer disease and amnestic mild cognitive impairment: A pilot clinical trial. Arch Neurol. 2012; 69:29–38. [PubMed: 21911655]

39. Whitman MC, Fan W, Rela L, Rodriguez-Gil DJ, Greer CA. Blood vessels form a migratory scaffold in the rostral migratory stream. J Comp Neurol. 2009; 516:94–104. [PubMed: 19575445]

40. Scranton RA, Fletcher L, Sprague S, Jimenez DF, Digicaylioglu M. The rostral migratory stream plays a key role in intranasal delivery of drugs into the CNS. PLoS One. 2011; 6:e18711. [PubMed: 21533252]

41. Grill JD, Cummings JL. Current therapeutic targets for the treatment of Alzheimer's disease. Expert Rev Neurother. 2010; 10:711–728. [PubMed: 20420492]

42. Oakley H, Cole SL, Logan S, Maus E, Shao P, Craft J, Guillozet-Bongaarts A, Ohno M, Disterhoft J, Van Eldik L, Berry R, Vassar R. Intraneuronal beta-amyloid aggregates, neurodegeneration, and

neuron loss in transgenic mice with five familial Alzheimer's disease mutations: Potential factors in amyloid plaque formation. J Neurosci. 2006; 26:10129–10140. [PubMed: 17021169]

43. Lacor PN, Buniel MC, Chang L, Fernandez SJ, Gong Y, Viola KL, Lambert MP, Velasco PT, Bigio EH, Finch CE, Krafft GA, Klein WL. Synaptic targeting by Alzheimer's-related amyloid beta oligomers. J Neurosci. 2004; 24:10191–10200. [PubMed: 15537891]
44. Gomez D, Martinez JA, Hanson LR, Frey WH 2nd, Toth CC. Intranasal treatment of neurodegenerative diseases and stroke. Front Biosci (Schol Ed). 2012; 4:74–89. [PubMed: 22202044]
45. Lochhead JJ, Thorne RG. Intranasal delivery of biologics to the central nervous system. Adv Drug Deliv Rev. 2012; 64:614–628. [PubMed: 22119441]
46. Costantino HR, Illum L, Brandt G, Johnson PH, Quay SC. Intranasal delivery: Physicochemical and therapeutic aspects. Int J Pharm. 2007; 337:1–24. [PubMed: 17475423]
47. Johnson NJ, Hanson LR, Frey WH. Trigeminal pathways deliver a low molecular weight drug from the nose to the brain and orofacial structures. Mol Pharm. 2010; 7:884–893. [PubMed: 20420446]
48. Curtis MA, Kam M, Nannmark U, Anderson MF, Axell MZ, Wikkelso C, Holtas S, van Roon-Mom WM, Bjork-Eriksson T, Nordborg C, Frisen J, Dragunow M, Faull RL, Eriksson PS. Human neuroblasts migrate to the olfactory bulb via a lateral ventricular extension. Science. 2007; 315:1243–1249. [PubMed: 17303719]
49. Sun W, Kim H, Moon Y. Control of neuronal migration through rostral migration stream in mice. Anat Cell Biol. 2010; 43:269–279. [PubMed: 21267400]
50. Kam M, Curtis MA, McGlashan SR, Connor B, Nannmark U, Faull RL. The cellular composition and morphological organization of the rostral migratory stream in the adult human brain. J Chem Neuroanat. 2009; 37:196–205. [PubMed: 19159677]
51. Eom TY, Li J, Anton ES. Going tubular in the rostral migratory stream: Neurons remodel astrocyte tubes to promote directional migration in the adult brain. Neuron. 2010; 67:173–175. [PubMed: 20670825]

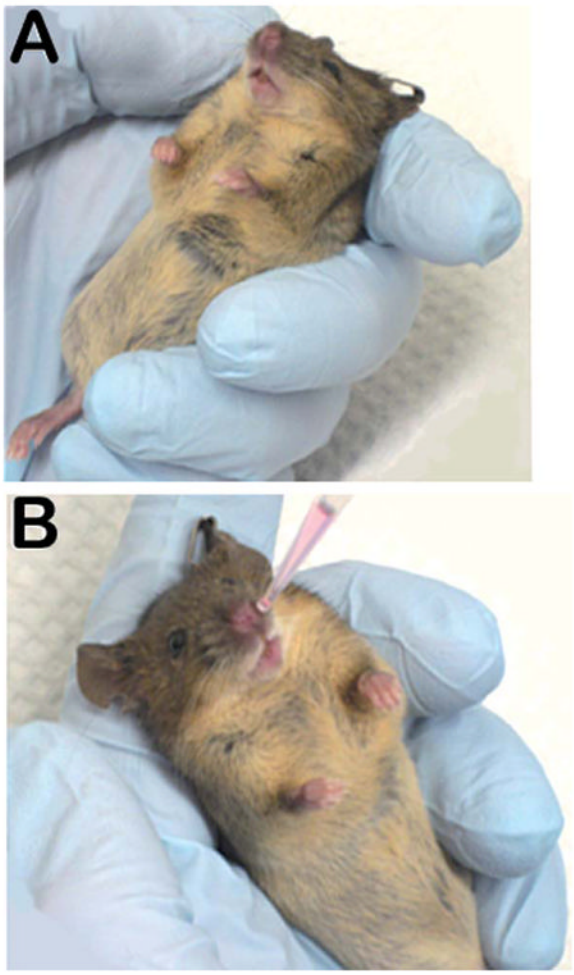

Fig. 1.
Representative photographs showing positioning of an anesthetized mouse (A) to be injected intranasally with the antibody using a microliter pipette-tip targeted over one naris (B).

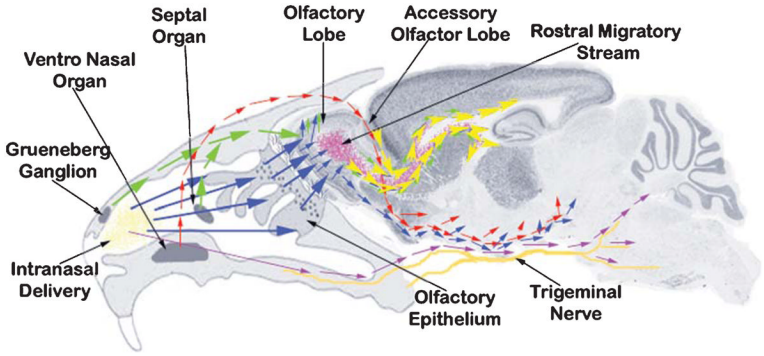

Fig. 2.

Schema showing major routes of entry utilized after intranasal delivery of therapeutics in mice. Intranasally administered material (yellow deposits) is picked up by sensory neurons of Grueneberg ganglion, septal organ (green arrows), olfactory epithelium (blue arrow), and ventro-nasal organ (red arrow). The sensory neurons of Grueneberg ganglion, septal organ (green arrows), and olfactory epithelium (blue arrow)—all projecting to the granule cells of the olfactory lobe—eventually drain intranasally-administered material into the rostral migratory stream (RMS) (yellow arrowheads) and olfactory track at the base of the mid-brain (blue and red arrows). The material tracked into the RMS reaches the lateral and 3rd ventricle in the close vicinity of hippocampus. The sensory neurons of ventro-nasal organ (red arrows) project to the accessory olfactory lobe, which further combine with the olfactory track at the base of the mid-brain. The material trafficked along the trigeminal nerve also combines with the olfactory track delivering to pons and hind brain, reaching to the 4th ventricle.

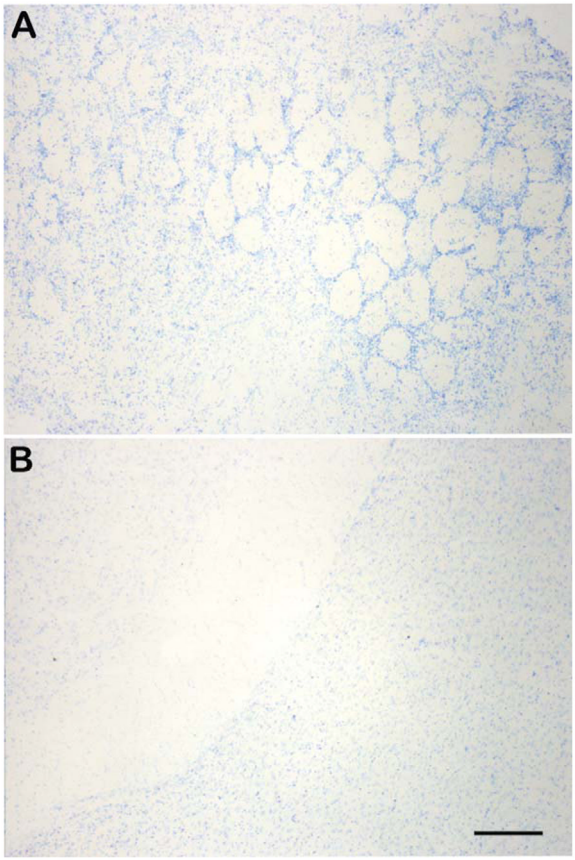

Fig. 3.

Representative photomicrographs showing absence of horseradish peroxidase labeling within the olfactory lobe parenchyma (A) and in the hippocampal vicinity (B) in the brains of saline vehicle injected mice at 12 h post-intranasal injection. Scale bar = 120 μm.

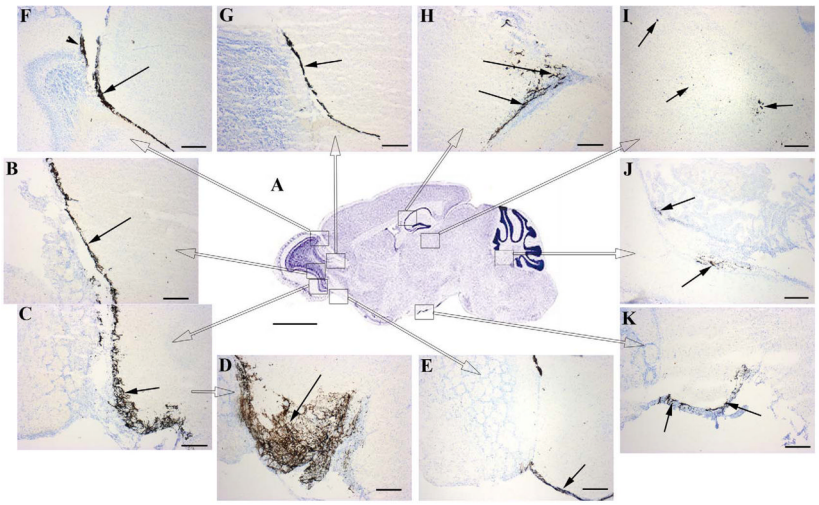

Fig. 4.

Representative photomicrographs showing transit of intranasally-delivered horseradish peroxidase (HRP) labeled NU4 antibody after a single bolus intransal injection at different time-points, tracked within different brain regions represented in the Nissl-stained sagittal section of mouse brain (A) as rectangular high power fields (C thru K). High power fields B and C (arrows) represent transit of HRP-NU4 through the glomerular and plexiform layers of olfactory lobe at 2 h post-intranasal injection, which was observed to be further advanced by 6 h post intranasal injection (D, arrow), progressing into the olfactory tract (E, arrow). At 6 h post intranasal injection, the HRP-NU4 antibody was found to enter accessory olfactory lobe (F, arrowhead) and rostral migratory stream (RMS) path (F, arrow). Trafficking into RMS was observed to progress further at 12 h post intranasal injection reaching the vicinity of hippocampus (arrows in H & I). HRP-NU4 was found to be transited in the olfactory-trigeminal path (K, arrows) leading to the 4th ventricle (J, arrows) at 12 h post injection. Scale bar in A = 1500 μm. Scale bars in C thru K = 150 μm.

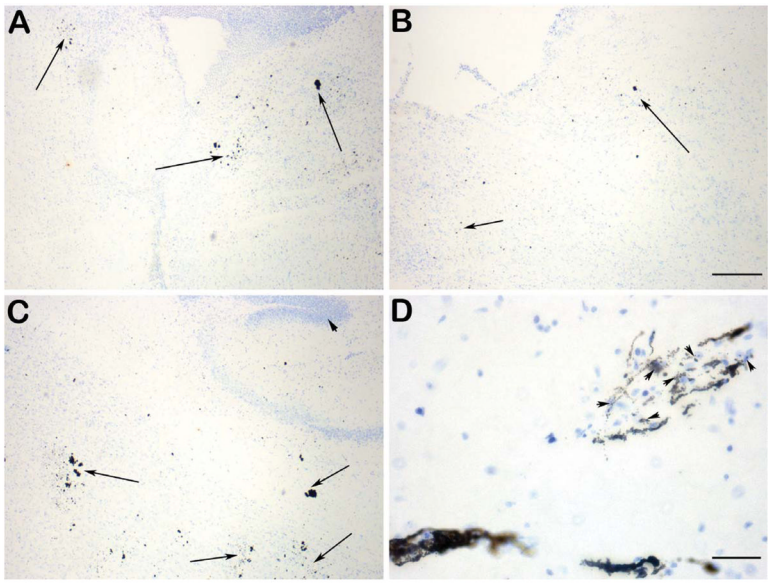

Fig. 5.

Representative photomicrographs showing brain parenchymal and neuronal uptake of HRP-NU4 at 6 h post intranasal injection in the vicinity of 3rd ventricle (A, arrows), midbrain (B, arrows), and hippocampus (C, arrows). High power magnification showing perikaryal uptake of NU4 (D, arrowheads). Scale bar in A thru C = 100 μm. Scale bar in D = 50 μm.

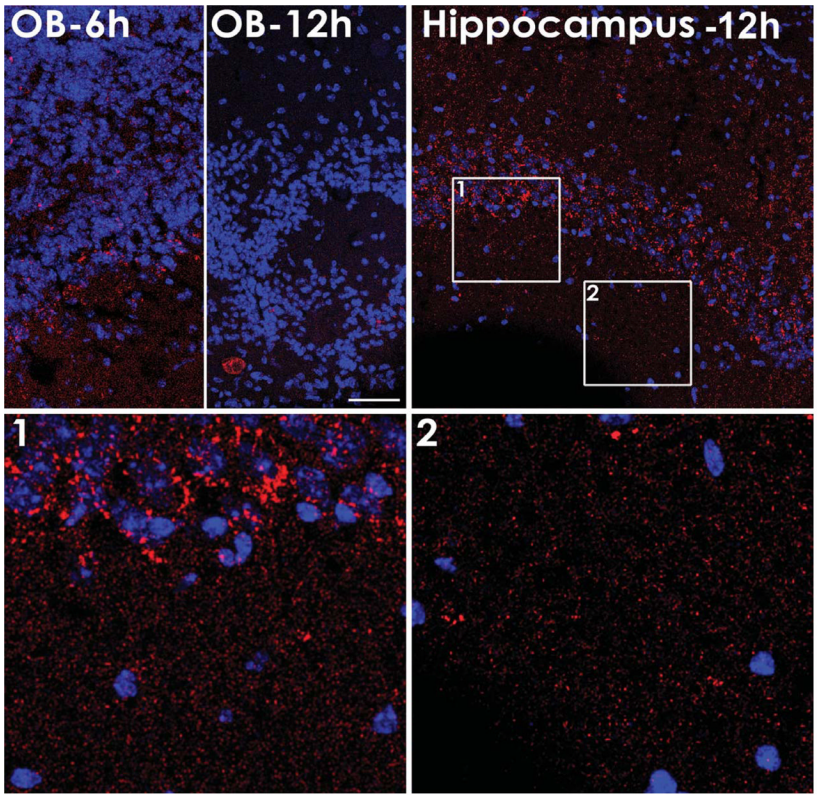

Fig. 6.

Distribution of fluorescently labeled NU4 at 6 and 12 h post injection showing detection of antibody within the olfactory bulb (OB) at 6 h (OB-6 h) or 12 h (OB-12 h) post-injection; and within the pyramidal neurons layer of the hippocampal CA1 region at 12 h post-injection (Hippocampus-12 h) showing perisomal labeling (Hippocampus-12 h, Panel 1, Panel 2). Scale bar = 50 μm.

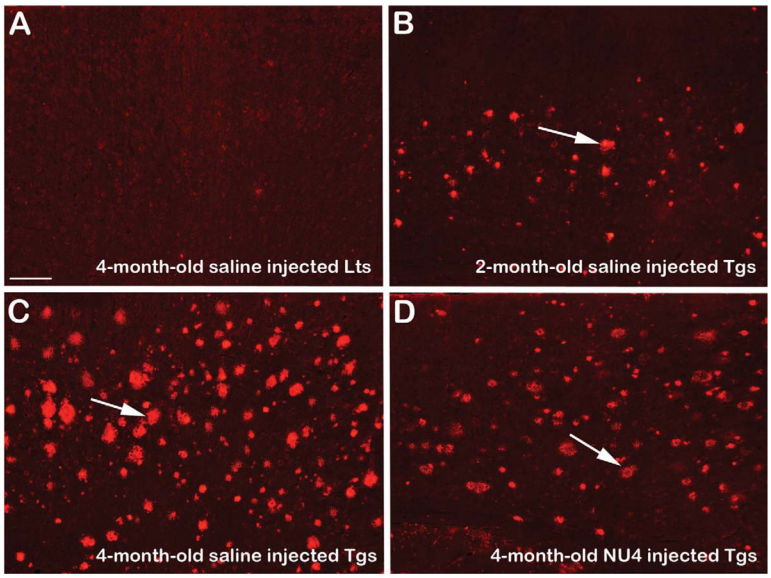

Fig. 7.

Representative photomicrographs showing the distribution of 6E10-immunoreactive (IR) Aβ plaques (arrows in B–D) within the cerebral cortex of 5XFAD mice. Note absence of 6E10-IR plaques in the brain of 4-month-old untreated age-matched saline injected non-transgenic littermates (Lts) (A). Note sparse distribution of 6E10-IR Aβ plaques in the brains of 2-month-old untreated saline injected control 5XFAD mice (Tgs) (B, arrow). Note significantly increased Aβ plaque load in the brains of 4-month-old untreated age-matched saline injected control 5XFAD mice (C, arrow). Note remarkable reduction of 6E10-IR Aβ plaques in the brains of 4-month-old 5XFAD mice intranasally immunized with NU4 (D, arrow). Scale bar = 60 μm.

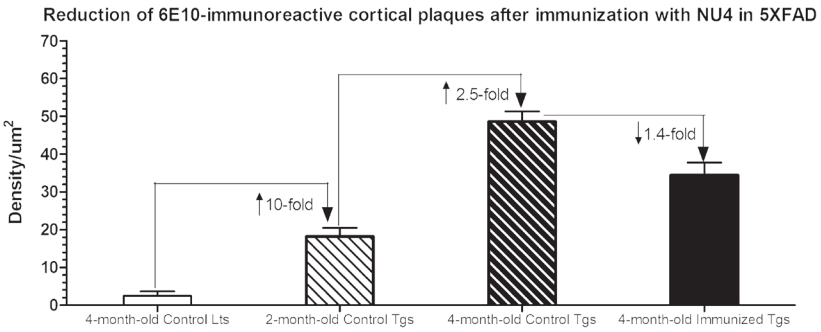

Fig. 8.

Densitometric quantitation of 6E10-immunoreactive (IR) plaques in 5XFAD brains before and after intranasal immunization with NU4 antibody. Note baseline density counts in 4-month-old untreated saline injected non-transgenic littermate (Lts) controls merely due to fluorescent background. Compared to littermate controls, the deposition of 6E10-IR Aβ plaques increased by ~10-fold in the brains of 2-month-old saline injected untreated control transgenic mice (Tgs), that were further increased by additional ~2.5-fold in the brains of 4-month-old saline injected age-matched untreated control transgenic mice. Intranasal immunization using NU4 significantly reduced 6E10-IR Aβ plaques by 1.4-fold in the brains of 4-month-old immunized 5XFAD mice (all values, $p < 0.0001$).

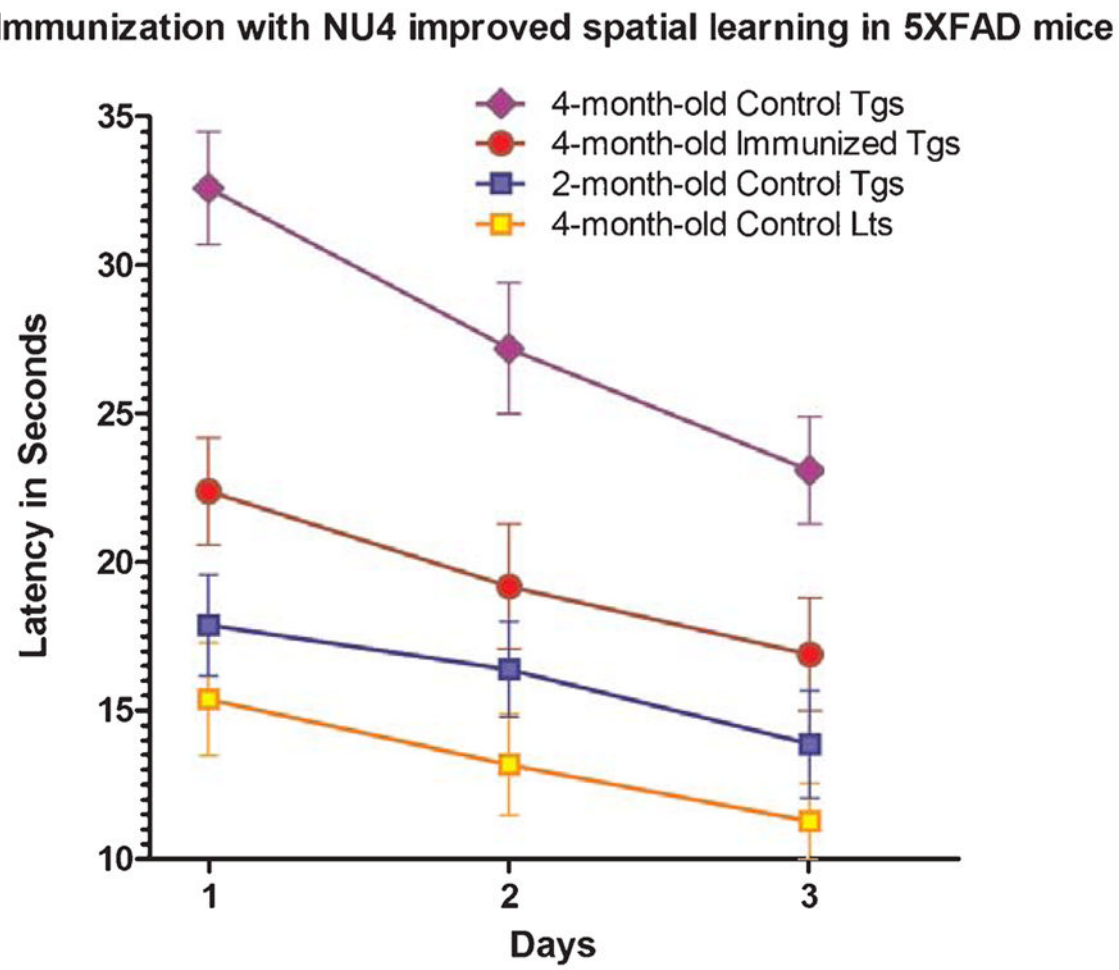

Fig. 9.

Effect of intranasal immunization on spatial acquisition learning in 5XFAD mice, as measured by latency (time in seconds required to reach the submerged platform in a given trial of 6 0 s duration) using Morris water maze apparatus. Data are represented as group means with standard deviation (SD) derived from the average individual values. Note least required latencies (8–15 s) by 4-month-old control littermates (Lts), with progressively increased latencies required by 2-month-old control transgenic (15–18 s) and 4-month-old control transgenic (25–31 s) mice (Tgs). Note that intranasal immunization with NU4 improved spatial acquisition learning as evidenced by reduced latencies (18–22 s) to reach the submerged platform compared to the latencies (25–31 s) required by age-matched control mice.